2022 IEEE 61st Conference on Decision and Control (CDC)
December 6-9, 2022. Cancún, Mexico

Stabilization of Nonholonomic Pendulum Skate by Controlled Lagrangians

Abstract— **We consider the problem of stabilizing what we call a pendulum skate, a simple model of a figure skater developed by Gzenda and Putkaradze. By exploiting the symmetry of the system as well as taking care of the part of the symmetry broken by the gravity, the equations of motion are given as nonholonomic Euler–Poincaré equation with advected parameters. Our main interest is the stability of the sliding and spinning equilibria of the system. We show that the former is unstable and the latter is stable only under certain conditions. We use the method of Controlled Lagrangians to find a control to stabilize the sliding equilibria.**

I. Introduction

The method of Controlled Lagrangians [17], [12], [13], [5], [2] is a successful nonlinear control technique for stabilizing mechanical systems described by the Euler–Lagrange equations. It has been extended to those mechanical systems on Lie groups with full symmetry using the Euler–Poincaré formalism [3], [7], [4], and also more recently to those with broken symmetry such as underwater vehicles [10], [9].

However, its extension to nonholonomic systems is limited to a very special class of Lagrange–d'Alembert equations [23], [24] (see also [6]). Also, to our knowledge, a further extension to nonholonomic Euler–Poincaré equations has been done only for a special case of the so-called Chaplygin sphere [21].

Developing a general method of controlled Lagrangian for nonholonomic systems is challenging for a couple of reasons: (i) The nonholonomic constraints complicate the resulting equations of motion due to the Lagrange multipliers arising from the constraints. (ii) The equations of motion are not in the Lagrangian/Hamiltonian form in the strict sense, although they are still energy-preserving.

II. Pendulum Skate

A. Basic Setup

This work is a step towards developing the method of Controlled Lagrangians for nonholonomic Euler–Poincaré equations. Particularly, we consider what we call the "pendulum skate" depicted in the Fig. 1. It is a simple model for a figure skater developed in [11], and consists of a skate—sliding without friction on the surface—with a pendulum rigidly attached to it.

Following [11], we would like to describe the system using a Lie group and exploit its symmetry so that the resulting equations of motion become a nonholonomic Euler–Poincaré equation after symmetry reduction.

Let $\{\boldsymbol{e}_1, \boldsymbol{e}_2, \boldsymbol{e}_3\}$ and $\{\boldsymbol{E}_1, \boldsymbol{E}_2, \boldsymbol{E}_3\}$ be the spatial (inertial and fixed) and the body (attached to the body) frame, respectively, where $\{\boldsymbol{E}_1, \boldsymbol{E}_2, \boldsymbol{E}_3\}$ is aligned with the principal axes of inertia with $\boldsymbol{E}_1$ being aligned with the edge of the blade as shown in Fig. 1. These two frames are related by the rotation matrix $R(t) \in \mathsf{SO}(3)$ whose column vectors represent the body frame viewed in the spatial one at time t. The origin of the body frame is the blade-ice contact point,

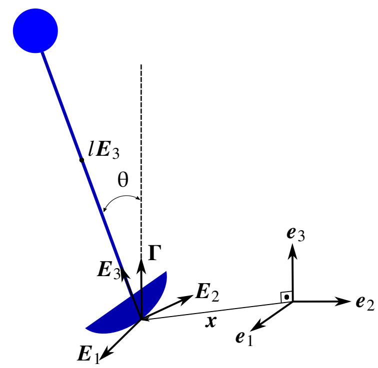

Fig. 1. Pendulum Skate

and has position vector $\boldsymbol{x}(t) = (x_1(t), x_2(t), 0)$ at time t in the spatial frame. Also in the body frame, the center of mass is located at $l\boldsymbol{E}_3$, which in spatial coordinates corresponds to $\boldsymbol{a}(t) = \boldsymbol{x}(t) + R(t) l \boldsymbol{E}_3$.

The configuration space is the semi-direct product Lie group $\mathsf{SE}(3) = \mathsf{SO}(3) \ltimes \mathbb{R}^3$, or the matrix group

$$\mathsf{SE}(3) = \left\{ (R, \boldsymbol{x}) := \begin{bmatrix} R & \boldsymbol{x} \\ \boldsymbol{0}^{\mathsf{T}} & 1 \end{bmatrix} : R \in \mathsf{SO}(3), \boldsymbol{x} \in \mathbb{R}^3 \right\}$$

under the standard matrix multiplication. However, the system does *not* possess the full $\mathsf{SE}(3)$-symmetry, because the gravity breaks the symmetry. To take this into account, we introduce the advected parameter $\boldsymbol{\Gamma} := R^{\mathsf{T}} \boldsymbol{e}_3$ (the opposite of the direction of gravity seen from the body frame), and θ is the angle between $\boldsymbol{E}_3$ and $\boldsymbol{e}_3$.

Let us find the Lagrangian of the system. If $t \mapsto \mathsf{g}(t) = (R(t), \boldsymbol{x}(t))$ is the dynamics of the system in $\mathsf{SE}(3)$, then

$$\mathsf{g}^{-1}\dot{\mathsf{g}} = \begin{bmatrix} R^{\mathsf{T}}\dot{R} & R^{\mathsf{T}}\dot{\boldsymbol{x}} \\ \boldsymbol{0}^{\mathsf{T}} & 0 \end{bmatrix} =: \begin{bmatrix} \widehat{\boldsymbol{\Omega}} & \boldsymbol{Y} \\ \boldsymbol{0}^{\mathsf{T}} & 0 \end{bmatrix} =: (\widehat{\boldsymbol{\Omega}}, \boldsymbol{Y}) \in \mathfrak{se}(3),$$

where $\widehat{\boldsymbol{\Omega}} := R^{\mathsf{T}}\dot{R}$ is the body angular velocity; $\boldsymbol{Y} := R^{\mathsf{T}}\dot{\boldsymbol{x}}$ is the velocity of the blade-ice contact point seen from the body frame; $\mathfrak{se}(3)$ is the Lie algebra of $\mathsf{SE}(3)$.

This work was supported by NSF grant CMMI-1824798.

J. Garcia and T. Ohsawa are with Department of Mathematical Sciences, The University of Texas at Dallas, 800 West Campbell Road, Richardson, TX 75080-3021, USA {jorge.garcia4,tomoki}@utdallas.edu

2022 IEEE 61st Conference on Decision and Control (CDC) | 978-1-6654-6761-2/22/$31.00 ©2022 IEEE | DOI: 10.1109/CDC51059.2022.9993264

Then, the Lagrangian $L\colon \mathsf{TSE}(3) \to \mathbb{R}$, defined on the tangent bundle $\mathsf{TSE}(3)$ of $\mathsf{SE}(3)$, is given by:

$$\begin{aligned} L(R, \boldsymbol{x}, \dot{R}, \dot{\boldsymbol{x}}) &:= \frac{1}{2}\operatorname{Tr}(\dot{R}\mathbb{J}\dot{R}^{\mathsf{T}}) + \frac{m}{2}\|\dot{\boldsymbol{a}}\|^2 - mg\boldsymbol{e}_3^{\mathsf{T}}\boldsymbol{a} \\ &= \frac{1}{2}\operatorname{Tr}(\widehat{\boldsymbol{\Omega}}\mathbb{J}\widehat{\boldsymbol{\Omega}}^{\mathsf{T}}) + \frac{m}{2}\left\|\boldsymbol{Y} + l\widehat{\boldsymbol{\Omega}}\boldsymbol{E}_3\right\|^2 - mgl\boldsymbol{\Gamma}^{\mathsf{T}}\boldsymbol{E}_3, \end{aligned}$$

where m is the total mass, g is the gravitational acceleration, $\|\boldsymbol{w}\| = \sqrt{\boldsymbol{w}^{\mathsf{T}}\boldsymbol{w}}$, $\forall \boldsymbol{w} \in \mathbb{R}^3$, and $\mathbb{J}$ is the inertia matrix.

Notice that the Lagrangian is written in terms of the variables $(\widehat{\boldsymbol{\Omega}}, \boldsymbol{Y}) \in \mathfrak{se}(3)$ as well as the advected parameter $\boldsymbol{\Gamma}$. Therefore, following [15], [8] and [16, §7.5], we may define the reduced extended Lagrangian $\ell\colon \mathfrak{se}(3) \times (\mathbb{R}^3)^* \to \mathbb{R}$:

$$\ell(\widehat{\boldsymbol{\Omega}}, \boldsymbol{Y}, \boldsymbol{\Gamma}) := K(\widehat{\boldsymbol{\Omega}}, \boldsymbol{Y}) - U(\boldsymbol{\Gamma}), \tag{1a}$$

with the kinetic energy $K\colon \mathfrak{se}(3) \to \mathbb{R}$ and the reduced potential $U\colon (\mathbb{R}^3)^* \to \mathbb{R}$ defined as

$$K(\widehat{\boldsymbol{\Omega}}, \boldsymbol{Y}) := \frac{1}{2}\operatorname{Tr}(\widehat{\boldsymbol{\Omega}}\mathbb{J}\widehat{\boldsymbol{\Omega}}^{\mathsf{T}}) + \frac{m}{2}\left\|\boldsymbol{Y} + \widehat{\boldsymbol{\Omega}}l\boldsymbol{E}_3\right\|^2, \tag{1b}$$

$$U(\boldsymbol{\Gamma}) := mg\boldsymbol{\Gamma}^{\mathsf{T}}l\boldsymbol{E}_3,$$

where we identify $(\mathbb{R}^3)^*$ with $\mathbb{R}^3$ via the dot product $\langle \boldsymbol{v}, \boldsymbol{w}\rangle := \boldsymbol{v}\cdot\boldsymbol{w}$ so that $\boldsymbol{\Gamma} \in (\mathbb{R}^3)^* \cong \mathbb{R}^3$.

We also identify $\boldsymbol{\Omega} = (\Omega_1, \Omega_2, \Omega_3) \in \mathbb{R}^3$ with $\widehat{\boldsymbol{\Omega}} \in \mathfrak{so}(3)$ via the hat map [16, §5.3]:

$$\widehat{(\bullet)}\colon \mathbb{R}^3 \to \mathfrak{se}(3); \qquad \boldsymbol{\Omega} \mapsto \widehat{\boldsymbol{\Omega}} = \begin{bmatrix} 0 & -\Omega_3 & \Omega_2 \\ \Omega_3 & 0 & -\Omega_1 \\ -\Omega_2 & \Omega_1 & 0 \end{bmatrix},$$

whose inverse is written as $(\bullet)^{\vee}\colon \mathfrak{so}(3) \to \mathbb{R}^3$. Then we have the following correspondence with the cross product: $\widehat{\boldsymbol{\Omega}}\mathbf{y} = \boldsymbol{\Omega} \times \mathbf{y}, \forall \mathbf{y} \in \mathbb{R}^3$. So we may use $(\boldsymbol{\Omega}, \boldsymbol{Y}) \in \mathbb{R}^3 \times \mathbb{R}^3$ as coordinates for $\mathfrak{se}(3) \cong \mathbb{R}^3 \times \mathbb{R}^3$, and we have $\frac{1}{2}\operatorname{Tr}(\widehat{\boldsymbol{\Omega}}\mathbb{J}\widehat{\boldsymbol{\Omega}}^{\mathsf{T}}) = \frac{1}{2}\boldsymbol{\Omega}^{\mathsf{T}}\mathbb{I}\boldsymbol{\Omega}$, where $\mathbb{I} = \operatorname{Tr}(\mathbb{J})\mathbb{1} - \mathbb{J} = \operatorname{diag}(I_1, I_2, I_3)$ is the (body) moment of inertia tensor, and $\mathbb{1}$ is the 3×3 identity matrix; see [16, §7.1].

As a result, we can rewrite the reduced Lagrangian (by notation abuse) as $\ell\colon \mathbb{R}^3 \times \mathbb{R}^3 \times \mathbb{R}^3 \to \mathbb{R}$, and (1) becomes:

$$\ell(\boldsymbol{\Omega}, \boldsymbol{Y}, \boldsymbol{\Gamma}) = K(\boldsymbol{\Omega}, \boldsymbol{Y}) - U(\boldsymbol{\Gamma}), \tag{2a}$$

$$K(\boldsymbol{\Omega}, \boldsymbol{Y}) := \frac{1}{2}\langle \mathbb{I}\boldsymbol{\Omega}, \boldsymbol{\Omega}\rangle + \frac{m}{2}\left\|\boldsymbol{Y} + l\boldsymbol{\Omega}\times\boldsymbol{E}_3\right\|^2, \tag{2b}$$

$$U(\boldsymbol{\Gamma}) := mgl\langle \boldsymbol{\Gamma}, \boldsymbol{E}_3\rangle, \tag{2c}$$

which agrees with [11]. Notice also

$$\dot{\boldsymbol{\Gamma}} = \frac{d}{dt}(R^{\mathsf{T}})\boldsymbol{e}_3 = -R^{\mathsf{T}}\dot{R}R^{\mathsf{T}}\boldsymbol{e}_3 = -\widehat{\boldsymbol{\Omega}}\boldsymbol{\Gamma} = -\boldsymbol{\Omega}\times\boldsymbol{\Gamma} = \boldsymbol{\Gamma}\times\boldsymbol{\Omega}$$

B. Constraints

The constraints considered in the model are [11]:

1) Pitch constancy: The blade does not rock back and forth.

$$\langle \boldsymbol{\Omega}, \boldsymbol{E}_1 \times \boldsymbol{\Gamma}\rangle = 0. \tag{3}$$

2) Continuous contact: The skate blade is in permanent contact with the plane of the ice, already addressed before by declaring $\boldsymbol{x}(t) = (x_1(t), x_2(t), 0)$, which means $\langle \boldsymbol{x}, \boldsymbol{e}_3\rangle = 0$. Taking the time derivative,

$$\langle \dot{\boldsymbol{x}}, \boldsymbol{e}_3\rangle = 0 \tag{4}$$

3) No side sliding: The skate blade moves without friction, but with a constraint that prohibits motions perpendicular to its edge.

$$\langle \dot{\boldsymbol{x}}, R\boldsymbol{E}_1 \times \boldsymbol{e}_3\rangle = 0. \tag{5}$$

Note that $\{\boldsymbol{E}_1, \boldsymbol{\Gamma}, \boldsymbol{E}_1\times\boldsymbol{\Gamma}\}$ forms an orthonormal frame (called the hybrid frame in [11]), and (4) says $\boldsymbol{Y} \perp \boldsymbol{\Gamma}$. So the above constraint says that the velocity $\boldsymbol{Y}$ of the contact point seen in the body frame must be aligned with the direction $\boldsymbol{E}_1$ along the edge of the blade, i.e.,

$$\boldsymbol{Y} = Y_1\boldsymbol{E}_1 + Y_2\boldsymbol{\Gamma} + Y_3\boldsymbol{E}_1\times\boldsymbol{\Gamma} = Y_1\boldsymbol{E}_1. \tag{6}$$

III. Equations of Motion (EOM)

A. Nonholonomic Euler–Poincaré Equation

The Lagrange–d'Alembert principle with the advected parameter $\boldsymbol{\Gamma}$ and the constraints (3)–(5) yields the **nonholonomic Euler–Poincaré equation** [21], [14, §12.3], [11]:

$$\begin{cases} \dfrac{d}{dt}\left(\dfrac{\partial\ell}{\partial\boldsymbol{\Omega}}\right) + \boldsymbol{\Omega}\times\dfrac{\partial\ell}{\partial\boldsymbol{\Omega}} + \boldsymbol{Y}\times\dfrac{\partial\ell}{\partial\boldsymbol{Y}} + \boldsymbol{\Gamma}\times\dfrac{\partial\ell}{\partial\boldsymbol{\Gamma}} = \lambda_1(\boldsymbol{E}_1\times\boldsymbol{\Gamma}), \\ \dfrac{d}{dt}\left(\dfrac{\partial\ell}{\partial\boldsymbol{Y}}\right) + \boldsymbol{\Omega}\times\dfrac{\partial\ell}{\partial\boldsymbol{Y}} = \lambda_2\boldsymbol{\Gamma} + \lambda_3(\boldsymbol{E}_1\times\boldsymbol{\Gamma}), \\ \dot{\boldsymbol{\Gamma}} = \boldsymbol{\Gamma}\times\boldsymbol{\Omega}. \end{cases} \tag{7}$$

Using the expression (2) for ℓ, incorporating the constraints(3)–(6), and eliminating the Lagrange multipliers, we obtain the following set of first order differential equations:

$$\dot{\Omega}_1 = \frac{ml(g\sin\theta + Y_1\Omega_3) + \Omega_3^2\tan\theta\left(ml^2 + I_2 - I_3\right)}{ml^2 + I_1}, \tag{8a}$$

$$\dot{\Omega}_3 = -\frac{\Omega_1\Omega_3\tan\theta\left(I_2\left(\sec^2\theta + 1\right) - I_3\right)}{I_2\tan^2\theta + I_3}, \tag{8b}$$

$$\dot{Y}_1 = -\frac{2lI_3\Omega_1\Omega_3\sec^2\theta}{I_2\tan^2(\theta) + I_3}, \tag{8c}$$

$$\dot{\theta} = \Omega_1 \tag{8d}$$

along with the algebraic relations

$$\Omega_2 = \Omega_3\tan(\theta), \quad Y_2 = Y_3 = 0, \quad \boldsymbol{\Gamma} = (0, \sin(\theta), \cos(\theta)). \tag{9}$$

IV. Equilibrium Points and Stability Analysis

A. Equilibrium Points

By setting $\dot{\Omega}_1 = \dot{\Omega}_3 = \dot{Y}_1 = \dot{\theta} = 0$ and solving the RHS of (8) for $(\Omega_1, \Omega_3, Y_1, \theta)$, we obtain a family of equilibrium points $(\boldsymbol{\Omega}_{\mathrm{e}}, \boldsymbol{Y}_{\mathrm{e}}, \boldsymbol{\Gamma}_{\mathrm{e}})$ with

$$\boldsymbol{\Omega}_{\mathrm{e}} = (0, \Omega_0\tan(\theta_0), \Omega_0), \quad \boldsymbol{Y} = (Y_0, 0, 0), \\ \boldsymbol{\Gamma}_{\mathrm{e}} = (0, \sin(\theta_0), \cos(\theta_0)),$$

where Ω_0, Y_0, θ_0 are constants satisfying:

$$Y_0\Omega_0 = -\frac{(ml^2 + I_2 - I_3)}{ml}\tan(\theta_0)\Omega_0^2 - g\sin(\theta_0).$$

For $\theta_0 = 0$, we have $Y_0\Omega_0 = 0$ yielding two special equilibrium points we are interested in: the sliding one, for $\Omega_0 = 0$; and the spinning one, for $Y_0 = 0$.

Let us write our equations of motion (8) as

$$\dot{z} = \boldsymbol{f}(z) \quad \text{with} \quad z := (\Omega_1, \Omega_3, Y_1, \theta). \tag{10}$$

The sliding equilibrium $(\boldsymbol{\Omega}, \boldsymbol{Y}, \theta) = (\boldsymbol{0}, Y_0\boldsymbol{E}_1, 0)$ for (10) is then

$$z_{\text{sl}} := (0, 0, Y_0, 0), \tag{11}$$

whereas the spinning equilibrium $(\boldsymbol{\Omega}, \boldsymbol{Y}, \theta) = (\Omega_0\boldsymbol{E}_3, \boldsymbol{0}, 0)$ for (8) is

$$z_{\text{sp}} := (0, \Omega_0, 0, 0). \tag{12}$$

B. Spinning Equilibrium

Proposition 1 (Stability of spinning equilibrium):

1) If $ml^2 + I_3 - I_2 < 0$, then the spinning equilibrium (11) is unstable.
2) If $ml^2 + I_3 - I_2 > 0$ and $\Omega_0 > \sqrt{mgl/(ml^2 + I_3 - I_2)}$, then the spinning equilibrium (11) is stable.

Proof: The Jacobian matrix at the spinning equilibrium (12) is

$$J_2 := J(z_{\text{sp}}) = \begin{pmatrix} 0 & 0 & \frac{ml\Omega_0}{ml^2+I_1} & \frac{mgl+\Omega_0^2\left(ml^2+I_2-I_3\right)}{ml^2+I_1} \\ 0 & 0 & 0 & 0 \\ -2l\Omega_0 & 0 & 0 & 0 \\ 1 & 0 & 0 & 0 \end{pmatrix}.$$

Its eigenvalues are

$$\left\{0, 0, \pm\sqrt{mgl - (ml^2 + I_3 - I_2)\Omega_0^2}\Big/\sqrt{ml^2 + I_1}\right\}.$$

If $ml^2 + I_3 - I_2 < 0$, then by the Instability from Linearization (***IL***) criterion [20, p.216], z_{sp} is unstable.

If $ml^2 + I_3 - I_2 > 0$, then the linear analysis is inconclusive, and so we would like to use the following nonlinear method:

Theorem 2 (The Energy–Casimir Theorem [1]): Consider a system of differential equations $\dot{z} = \boldsymbol{f}(z)$ on $\mathbb{R}^n$ with f locally Lipschitz and $\boldsymbol{f}(\boldsymbol{p}) = \boldsymbol{0}$. Assume that the system has $k < n$ constants of motion $h_j(z)$, $j = 1, \ldots, k$. Let each h_j be C^2 and submersive at $\boldsymbol{p}$. Assume that the vectors $\nabla h_j(z)$, $j = 2, \ldots, k$ are linearly independent at $\boldsymbol{p}$. Then $\boldsymbol{p}$ is a stable equilibrium point if there exist scalars $\mu_2 \ldots, \mu_k$ such that:

(i) $h_1 + \mu_2 h_2 + \cdots + \mu_k h_k$ is critical at $\boldsymbol{p}$; and
(ii) the Hessian matrix $D^2(h_1 + \mu_2 h_2 + \cdots + \mu_k h_k)(\boldsymbol{p})$ is sign definite for all vectors belonging to the tangent space $\{\boldsymbol{y} \in \mathbb{R}^n \colon \nabla h_j(\boldsymbol{p}) \cdot \boldsymbol{y} = 0, j = 2, \ldots, k\}$ at $\boldsymbol{p}$ of the submanifold defined by $h_j(z) = h_j(\boldsymbol{p})$, $j = 2, \ldots, k$.

We also note that, despite its name, the above theorem does not assume that the constants of motion $\{h_j\}_{j=2}^k$ are Casimirs: any constants of motion—Casimirs or not—would suffice.

Imposing the algebraic relations (9) or equivalently

$$\boldsymbol{\Omega} = (\Omega_1, \Omega_3 \tan(\theta), \Omega_3), \quad \boldsymbol{Y} = (Y_1, 0, 0),$$
$$\boldsymbol{\Gamma} = (0, \sin(\theta), \cos(\theta)),$$

the kinetic and potential energies (2b) and (2c) become

$$K_{\text{r}}(\Omega_1, \Omega_3, Y_1) := \frac{1}{2}\Big(I_2\Omega_3^2 \tan^2(\theta) + I_1\Omega_1^2 + I_3\Omega_3^2 + m\big(l^2\Omega_1^2 + (l\Omega_3 \tan(\theta) + Y_1)^2\big)\Big),$$
$$U_{\text{r}}(\theta) = mgl\cos(\theta).$$

Set

$$h_1 := K_{\text{r}} + U_{\text{r}}, \qquad h_2 := (I_3\cos(\theta) + I_2\sin(\theta)\tan(\theta))\Omega_3,$$

it can be verified that the derivatives of h_1 and h_2 vanish along the vector field $\boldsymbol{f}(z)$, hence we just found two constants of motion. Writing $\Omega_3 = h_2/(I_3\cos(\theta) + I_2\sin(\theta)\tan(\theta))$, and substituting this into (8c)÷(8d), we obtain:

$$\frac{dY_1}{d\theta} = \frac{\dot{Y}_1}{\dot{\theta}} = -\frac{2h_2 l I_3 \sec^3(\theta)}{\left(I_2\tan^2(\theta) + I_3\right)^2},$$
$$Y_1 + 2h_2 l I_3 \int \frac{\sec^3(\theta)\, d\theta}{\left(I_2\tan^2(\theta) + I_3\right)^2} = \text{Const.} =: h_3,$$
$$h_3 = Y_1 + l\Omega_3\Big(G(\theta) + \tan(\theta)\Big),$$
$$G(\theta) := \frac{\cos(\theta)\,\left(I_2\tan^2(\theta) + I_3\right)\tan^{-1}\left(\frac{\sqrt{I_2 - I_3}\sin(\theta)}{\sqrt{I_3}}\right)}{\sqrt{I_2 - I_3}\sqrt{I_3}}.$$

Notice that G is real-valued because we are assuming $I_2 - I_3 > 0$, which is reasonable with the geometry of the system; see Fig. 1.

One can check that the derivative of h_3 vanishes along the vector field $\boldsymbol{f}(z)$. Also, since

$$\nabla h_1(z_{\text{sp}}) = (0, \Omega_0 I_3, 0, 0),$$
$$\nabla h_2(z_{\text{sp}}) = (0, I_3, 0, 0), \quad \nabla h_3(z_{\text{sp}}) = (0, 0, 1, 2l\Omega_0),$$

setting $\mu_2 = -\Omega_0$ and $\mu_3 = 0$, we have

$$\nabla(h_1 + \mu_2 h_2 + \mu_3 h_3)(z_{\text{sp}}) = \boldsymbol{0}$$

as well as

$$\mathsf{H}_{\Omega_0} := D^2(h_1 + \mu_2 h_2(z) + \mu_3 h_2)(z_{\text{sp}}) = \begin{pmatrix} ml^2 + I_1 & 0 & 0 & 0 \\ 0 & I_3 & 0 & 0 \\ 0 & 0 & m & ml\Omega_0 \\ 0 & 0 & ml\Omega_0 & \Omega_0^2\left(ml^2 + I_3 - I_2\right) - mgl \end{pmatrix}.$$

The relevant tangent space is the null space of the matrix

$$\ker\begin{pmatrix} \nabla h_2(z_{\text{sp}})^\top \\ \nabla h_3(z_{\text{sp}})^\top \end{pmatrix} = \ker\begin{pmatrix} 0 & I_3 & 0 & 0 \\ 0 & 0 & 1 & 2l\Omega_0 \end{pmatrix} = \left\{\boldsymbol{y} = (s_1, 0, -2l\Omega_0 s_2, s_2)^\top \mid s_1, s_2 \in \mathbb{R}\right\}.$$

Hence we have the quadratic form

$$\boldsymbol{y}^\top \mathsf{H}_{\Omega_0}\boldsymbol{y} = s_1^2(ml^2 + I_1) + s_2^2\left[\Omega_0^2(ml^2 + I_3 - I_2) - mgl\right],$$

which is positive definite in $(s_1, s_2)^\top$ for the assumed conditions $ml^2 + I_3 - I_2 > 0$ and $\Omega_0 > \sqrt{mgl/(ml^2 + I_3 - I_2)}$. ■

C. Sliding Equilibrium

Proposition 3 (Stability of sliding equilibrium): The sliding equilibrium (11) is linearly unstable.

Proof: Calculating the Jacobian matrix $J(z)$ of the RHS of (10) at the sliding equilibrium $z = z_{\rm sl}$ from (11),

$$J_1 := J(z_{\rm sl}) = \begin{pmatrix} 0 & \frac{mlY_0}{ml^2+I_1} & 0 & \frac{mgl}{ml^2+I_1} \\ 0 & 0 & 0 & 0 \\ 0 & 0 & 0 & 0 \\ 1 & 0 & 0 & 0 \end{pmatrix}.$$

Its eigenvalues are $\left\{0, 0, \pm\sqrt{mgl}/\sqrt{ml^2+I_1}\right\}$, and the presence of a positive eigenvalue implies the assertion by the ***IL*** criterion. ■

V. Stabilization by Controlled Lagrangian

A. Pendulum Skate Controlled by Rotor

We would like to stabilize the unstable sliding equilibrium $(\boldsymbol{\Omega}, \boldsymbol{Y}, \theta) = (\boldsymbol{0}, Y_0\boldsymbol{E}_1, 0)$ by the method of Controlled Lagrangians. Particularly, as is done in [21] for the Chaplygin sphere, we apply the control by a rotor with rotation axis parallel to $\boldsymbol{E}_1$ and attached to the center of mass of the pendulum skate, as depicted in Fig. 2.

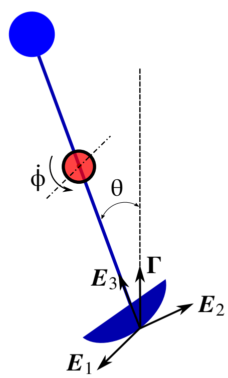

Fig. 2. Control Rotor attached to Pendulum Skate

The configuration space becomes $\mathbb{S}^1 \times \mathsf{SE}(3)$, where $\mathbb{S}^1$ refers to the rotor angle measured relative to the body frame, denoted by ϕ. Letting m denote the total mass of pendulum skate *including the rotor*, the only change in the Lagrangian is in the rotational energy:

$$K_{\rm rot} := \frac{1}{2}\left(I_1\Omega_1^2 + J_1(\Omega_1 + \dot\phi)^2 + \sigma_2\Omega_2^2 + \sigma_3\Omega_3^2\right),$$

where $\sigma_i := I_i + J_i$ with J_i $(i = 1, 2, 3)$ being the moments of inertia of the rotor with principal axes aligned with those of the pendulum skate. The new reduced Lagrangian $\ell_0 : \mathbb{S}^1 \times \mathbb{R}^3 \times \mathbb{R}^3 \times \mathbb{R}^3 \to \mathbb{R}$ is

$$\ell_0(\phi, \boldsymbol{\Omega}, \boldsymbol{Y}, \boldsymbol{\Gamma}) := K_{\rm rot} + \frac{m}{2}\|\boldsymbol{Y} + l\boldsymbol{\Omega}\times\boldsymbol{E}_3\|^2 - U(\boldsymbol{\Gamma}).$$

Notice that the Lagrangian ℓ_0 is independent of ϕ, and also that the variation $\delta\phi$ is independent of any of the variations $\delta\boldsymbol{\Omega}$, $\delta\boldsymbol{Y}$, $\delta\boldsymbol{\Gamma}$, δR, $\delta\boldsymbol{x}$. Hence the procedure from Section III-A produces the same equations (7) with ℓ being replaced by ℓ_0:

$$\begin{cases} \frac{d}{dt}\left(\frac{\partial\ell_0}{\partial\boldsymbol{\Omega}}\right) + \boldsymbol{\Omega}\times\frac{\partial\ell_0}{\partial\boldsymbol{\Omega}} + \boldsymbol{Y}\times\frac{\partial\ell_0}{\partial\boldsymbol{Y}} + \boldsymbol{\Gamma}\times\frac{\partial\ell_0}{\partial\boldsymbol{\Gamma}} = \lambda_1(\boldsymbol{E}_1\times\boldsymbol{\Gamma}), & (13a) \\ \frac{d}{dt}\left(\frac{\partial\ell_0}{\partial\boldsymbol{Y}}\right) + \boldsymbol{\Omega}\times\frac{\partial\ell_0}{\partial\boldsymbol{Y}} = \lambda_2\boldsymbol{\Gamma} + \lambda_3(\boldsymbol{E}_1\times\boldsymbol{\Gamma}), & (13b) \\ \dot{\boldsymbol{\Gamma}} = \boldsymbol{\Gamma}\times\boldsymbol{\Omega}. & (13c) \end{cases}$$

Assuming that a control torque u is applied to the new ϕ part of the equation, we also have

$$\frac{d}{dt}\left(\frac{\partial\ell_0}{\partial\dot\phi}\right) = u \Rightarrow \frac{d}{dt}J_1(\dot\phi + \Omega_1) = u. \tag{13d}$$

B. Controlled Lagrangian

The method of Controlled Lagrangians consists of finding a new Lagrangian $\ell_\nu : \mathbb{S}^1 \times \mathbb{R}^3 \times \mathbb{R}^3 \times \mathbb{R}^3 \to \mathbb{R}$ such that the Euler–Poincaré equation for ℓ_ν without control matches the above controlled equation (13). Specifically, we follow [21] and consider the following family of Lagrangians parameterized by $\nu \in \mathbb{R}$:

$$\begin{aligned} \ell_\nu &= K_\nu + \frac{m}{2}\|\boldsymbol{Y} + l\Omega\times\boldsymbol{E}_3\|^2 + U(\boldsymbol{\Gamma}), \\ K_\nu &= \frac{1}{2}\left(\frac{J_1}{1+\nu}\dot\phi^2 + 2J_1\Omega_1\dot\phi + \sigma_1\Omega_1^2 + \sigma_2\Omega_2^2 + \sigma_3\Omega_3^2\right). \end{aligned} \tag{14}$$

The Euler–Poincaré equation for ℓ_ν is the same as (13a) and (13c) with ℓ_0 being replaced by ℓ_ν:

$$\begin{cases} \frac{d}{dt}\left(\frac{\partial\ell_\nu}{\partial\boldsymbol{\Omega}}\right) + \boldsymbol{\Omega}\times\frac{\partial\ell_\nu}{\partial\boldsymbol{\Omega}} + \boldsymbol{Y}\times\frac{\partial\ell_\nu}{\partial\boldsymbol{Y}} + \boldsymbol{\Gamma}\times\frac{\partial\ell_\nu}{\partial\boldsymbol{\Gamma}} = \lambda_1(\boldsymbol{E}_1\times\boldsymbol{\Gamma}), & (15a) \\ \frac{d}{dt}\left(\frac{\partial\ell_\nu}{\partial\boldsymbol{Y}}\right) + \boldsymbol{\Omega}\times\frac{\partial\ell_\nu}{\partial\boldsymbol{Y}} = \lambda_2\boldsymbol{\Gamma} + \lambda_3(\boldsymbol{E}_1\times\boldsymbol{\Gamma}), & (15b) \\ \dot{\boldsymbol{\Gamma}} = \boldsymbol{\Gamma}\times\boldsymbol{\Omega}. & (15c) \end{cases}$$

with only significant change in (15d):

$$\begin{aligned} \frac{d}{dt}\left(\frac{\partial\ell_\nu}{\partial\dot\phi}\right) = 0 &\Rightarrow \frac{d}{dt}J_1(\dot\phi + (1+\nu)\Omega_1) = 0 \\ &\Rightarrow \frac{d}{dt}J_1(\dot\phi + \Omega_1) = -\nu J_1\dot\Omega_1. \end{aligned} \tag{15d}$$

The equations (15) match the controlled ones (13) by setting the rotor torque as $u = -\nu J_1\dot\Omega_1$. One sees in (15d) that the momentum $\partial\ell_\nu/\partial\dot\phi$ is constant; hence we can assume the rotor starts with no momentum of its own relative to the pendulum skate:

$$\frac{\partial\ell_\nu}{\partial\dot\phi} = 0 \Rightarrow \dot\phi = -(1+\nu)\Omega_1.$$

Substituting this into (14) yields:

$$K_\nu = \frac{1}{2}\left((I_1 - \nu J_1)\Omega_1^2 + \sigma_2\Omega_2^2 + \sigma_3\Omega_3^2\right) = \frac{1}{2}\boldsymbol{\Omega}^{\mathsf{T}}\mathbb{I}_\nu\,\boldsymbol{\Omega}$$

with

$$\mathbb{I}_\nu := \mathsf{diag}(\sigma_\nu, \sigma_2, \sigma_3) \quad \text{with} \quad \sigma_\nu := I_1 - \nu J_1, \tag{16}$$

and so the controlled Lagrangian becomes

$$\ell_\nu = \frac{1}{2}\boldsymbol{\Omega}^{\mathsf{T}}\mathbb{I}_\nu\,\boldsymbol{\Omega} + \frac{m}{2}\|\boldsymbol{Y} + l\boldsymbol{\Omega}\times\boldsymbol{E}_3\|^2 - U(\boldsymbol{\Gamma}).$$

Notice that it is identical to (2) except the moment of inertia $\mathbb{I}$ is replaced by $\mathbb{I}_\nu$. Therefore, we may eliminate the Lagrange multipliers and obtain a reduced set of EOM without multipliers just as before: we just have to replace (I_1, I_2, I_3) by $(\sigma_\nu, \sigma_2, \sigma_3)$:

$$\begin{cases} \dot{\Omega}_1 = \dfrac{ml\left(g\sin\theta + Y_1\Omega_3\right) + \Omega_3^2\tan\theta\left(ml^2 + \sigma_2 - \sigma_3\right)}{ml^2 + \sigma_\nu}, \\ \dot{\Omega}_3 = -\dfrac{\Omega_1\Omega_3\tan\theta\left(\sigma_2\left(\sec^2\theta + 1\right) - \sigma_3\right)}{\sigma_2\tan^2\theta + \sigma_3}, \\ \dot{Y}_1 = -\dfrac{2l\sigma_3\Omega_1\Omega_3\sec^2\theta}{\sigma_2\tan^2\theta + \sigma_3}, \\ \dot{\theta} = \Omega_1. \end{cases} \tag{17}$$

We write this system as

$$\dot{z} = f_\nu(z) \quad \text{with} \quad z := (\Omega_1, \Omega_3, Y_1, \theta).$$

Notice that the sliding equilibrium $z_{\rm sl}$ from (11) is an equilibrium of this system as well.

C. Stabilization of Sliding Equilibrium

Theorem 4 (Stabilization of sliding equilibrium): For the controlled pendulum skate (17), the sliding equilibrium (11) is stabilized if

$$\nu > \frac{ml^2 + I_1}{J_1}. \tag{18}$$

Proof: Let us set

$$\begin{aligned} K_{\nu r}(\Omega_1, \Omega_3, Y_1) &:= \frac{1}{2}\Big(\sigma_2\Omega_3^2\tan^2\theta + \sigma_\nu\Omega_1^2 + \sigma_3\Omega_3^2 + \\ &\qquad + m\left(l^2\Omega_1^2 + (l\Omega_3\tan\theta + Y_1)^2\right)\Big), \\ U_{\nu r}(\theta) &:= mgl\cos\theta, \\ h_1 &:= K_{\nu r} + U_{\nu r}, \\ h_2 &:= (\sigma_3\cos\theta + \sigma_2\sin\theta\tan\theta)\Omega_3, \\ h_3 &:= Y_1 + l\Omega_3\Big(G(\theta) + \tan\theta\Big), \\ G(\theta) &:= \frac{\cos\theta\left(\sigma_2\tan^2\theta + \sigma_3\right)\tan^{-1}\left(\frac{\sqrt{\sigma_2 - \sigma_3}\sin\theta}{\sqrt{\sigma_3}}\right)}{\sqrt{\sigma_2 - \sigma_3}\sqrt{\sigma_3}}. \end{aligned}$$

Notice that G is real-valued because we are assuming $J_2 = J_3$ (see Fig. 2), which implies $\sigma_2 - \sigma_3 = I_2 - I_3 > 0$.

Then h_1, h_2, h_3 are constants of motion. So we again use Theorem 2 along with these invariants. Since

$$\nabla h_1(z_{\rm sl}) = (0, 0, mY_0, 0),$$
$$\nabla h_2(z_{\rm sl}) = (0, \sigma_3, 0, 0), \quad \nabla h_3(z_{\rm sl}) = (0, 0, 1, 0),$$

setting $\mu_2 = 0$ and $\mu_3 = -mY_0$, we have

$$\nabla(h_1 + \mu_2 h_2 + \mu_3 h_3)(z_{\rm sl}) = \mathbf{0}$$

as well as

$$\begin{aligned} \mathsf{H}_{Y_0} &:= D^2(h_1 + \mu_2 h_2 + \mu_3 h_2)(z_{\rm sl}) \\ &= \begin{pmatrix} l^2 m + \sigma_\nu & 0 & 0 & 0 \\ 0 & \sigma_3 & 0 & -mlY_0 \\ 0 & 0 & m & 0 \\ 0 & -mlY_0 & 0 & -mgl \end{pmatrix}. \end{aligned}$$

The relevant tangent space is the null space of the matrix

$$\begin{aligned} \ker\begin{pmatrix} \nabla h_2(z_{\rm sl})^{\mathsf{T}} \\ \nabla h_3(z_{\rm sl})^{\mathsf{T}} \end{pmatrix} &= \begin{pmatrix} 0 & \sigma_3 & 0 & 0 \\ 0 & 0 & 1 & 0 \end{pmatrix} \\ &= \left\{ \boldsymbol{y} = (s_1, 0, 0, s_2)^{\mathsf{T}} \mid s_1, s_2 \in \mathbb{R} \right\}. \end{aligned}$$

Hence we have the quadratic form

$$\boldsymbol{y}^{\mathsf{T}}\mathsf{H}_{Y_0}\boldsymbol{y} = (ml^2 + \sigma_\nu)s_1^2 - mgls_2^2,$$

which is negative definite in $(s_1, s_2)^{\mathsf{T}}$ if $ml^2 + \sigma_\nu < 0$ or equivalently (18) in view of (16). ■

VI. Simulations

As a numerical example, consider the pendulum skate with mass $m = 2.00$ [Kg], $l = 0.80$ [m], $g = 9.80$ [m $\cdot$ s^{-2}], $\mathbb{I} = \mathrm{diag}(0.35, 0.35, 0.004)$ [Kg $\cdot$ m^2].

A. Sliding Equilibrium—Uncontrolled

For the sliding equilibrium $(\boldsymbol{\Omega} = \mathbf{0}, \boldsymbol{Y} = Y_0\boldsymbol{E}_1, \theta = 0)$, we select an initial condition with a small perturbation as follows:

$$\begin{aligned} \boldsymbol{\Omega}(0) = (0.1, 0.1\tan(0.1), 0.1), \quad \boldsymbol{Y}(0) = (1, 0, 0), \\ \boldsymbol{\Gamma}(0) = (0, \sin(0.1), \cos(0.1)), \end{aligned} \tag{19}$$

Figure 3 shows the result of the simulation of the uncontrolled system (8) with the above initial condition. It clearly exhibits instability as the pendulum skate falls down, i.e., $\Gamma_2 = 1$ at $T = 1.025$ [s].

B. Sliding Equilibrium—Controlled

We also solved the controlled system (17) with the same initial condition (19). For this simulation, the rotor mass is 1 [Kg], hence the total mass is $m = 3$ [Kg], $J_1 = 0.005$ [Kg $\cdot$ m^2], $J_2 = J_3 = 0.0025$ [Kg $\cdot$ m^2]. According to (18), the control parameter ν must satisfy $\nu > 454$ for stability; hence we take $\nu = 500$.

Figure 4 shows the result of the simulation. Notice that the solution stays close to the equilibrium with small oscillations, indicating that the pendulum skate keeps sliding without falling.

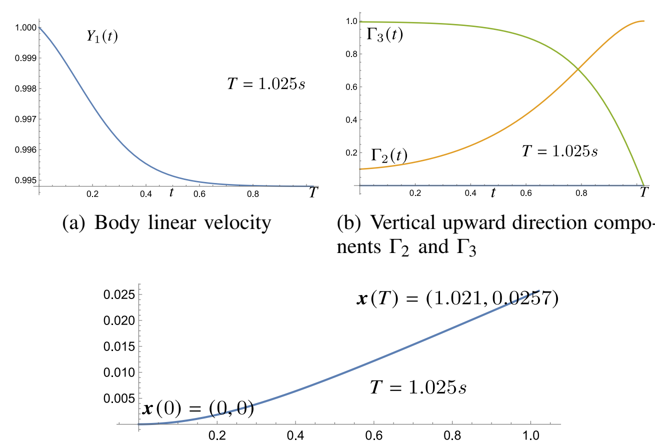

(a) Body linear velocity

(b) Vertical upward direction components Γ_2 and Γ_3

(c) Blade trajectory

Fig. 3. Uncontrolled dynamics.

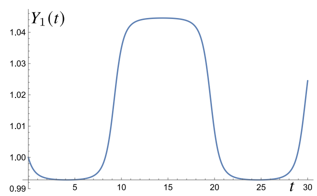

(a) Body linear velocity

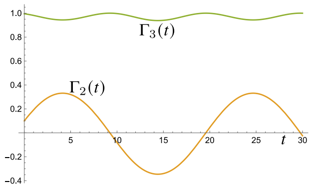

(b) Vertical upward direction components Γ_2 and Γ_3

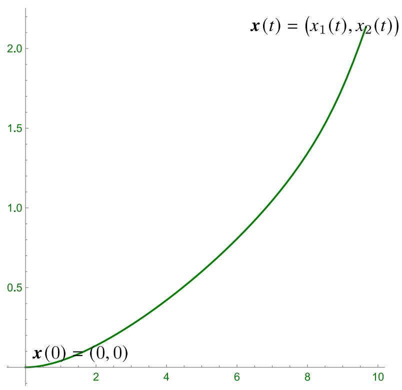

(c) Blade trajectory

Fig. 4. Controlled dynamics.

VII. Conclusion and Future Works

A. Conclusion

We analyzed the stability of the pendulum skate—a simple model of a figure skater developed by [11]. Specifically, we built on their model and derived the reduced set of equations (8) without Lagrange multipliers. We found the equilibrium points corresponding to the sliding and spinning of the figure skater, and analyzed their stability. Finally, we found a control that stabilizes unstable sliding equilibria by the method of Controlled Lagrangians.

B. Future Works

This work is our first step towards a more general treatment of Controlled Lagrangians applied to nonholonomic Euler–Poincaré equations with broken symmetry. Our goal in future works is to extend our previous works [9], [10] on Euler–Poincaré equations with broken symmetry to those with nonholonomic constraints. Also, the proposed control by the Controlled Lagrangian method only sought stability in the sense of Lyapunov. In future studies, we will seek asymptotic stability by applying an additional dissipative control, possibly switching to the Hamiltonian picture and using the IDA-PBC formalism [19], [18], [22].

VIII. Acknowledgments

The authors gratefully thank Vakhtang Putkaradze for helpful discussions, and the reviewers for their comments and suggestions.

References

[1] D. Aeyels. On stabilization by means of the Energy–Casimir method. *Systems & Control Letters*, 18(5):325–328, 1992.

[2] A. M. Bloch, D. E. Chang, N. E. Leonard, and J. E. Marsden. Controlled Lagrangians and the stabilization of mechanical systems. II. Potential shaping. *IEEE Transactions on Automatic Control*, 46(10):1556–1571, Oct 2001.

[3] A. M. Bloch, P. S. Krishnaprasad, J. E. Marsden, and G. Sánchez de Alvarez. Stabilization of rigid body dynamics by internal and external torques. *Automatica*, 28(4):745–756, 1992.

[4] A. M. Bloch, N. E. Leonard, and J. E. Marsden. Controlled Lagrangians and the stabilization of Euler–Poincaré mechanical systems. *International Journal of Robust and Nonlinear Control*, 11(3):191–214, 2001.

[5] A. M. Bloch, N. E. Leonard, and J. E. Marsden. Controlled Lagrangians and the stabilization of mechanical systems. I. The first matching theorem. *IEEE Transactions on Automatic Control*, 45(12):2253–2270, Dec 2000.

[6] A. M. Bloch, M. Reyhanoglu, and N. H. McClamroch. Control and stabilization of nonholonomic dynamic systems. *IEEE Transactions on Automatic Control*, 37(11):1746–1757, 1992.

[7] A. M. Bloch, D. E. Chang, N. E. Leonard, J. E. Marsden, and C. Woolsey. Asymptotic stabilization of Euler–Poincaré mechanical systems. *IFAC Proceedings Volumes*, 33(2):51–56, 2000.

[8] H. Cendra, D. D. Holm, J. E. Marsden, and T. S. Ratiu. Lagrangian reduction, the Euler–Poincaré equations, and semidirect products. *Amer. Math. Soc. Transl.*, 186:1–25, 1998.

[9] C. Contreras and T. Ohsawa. Controlled Lagrangians and stabilization of Euler–Poincaré mechanical systems with broken symmetry I: Kinetic shaping. *SIAM Journal on Control and Optimization*, 60(5):2684–2711, 2022.

[10] C. Contreras and T. Ohsawa. Controlled Lagrangians and stabilization of Euler–Poincaré mechanical systems with broken symmetry II: potential shaping. *Mathematics of Control, Signals, and Systems*, 34(2):329–359, 2022.

[11] V. Gzenda and V. Putkaradze. Integrability and chaos in figure skating. *Journal of Nonlinear Science*, 30(3):831–850, 2020.

[12] J. Hamberg. General matching conditions in the theory of controlled Lagrangians. *Decision and Control, 1999. Proceedings of the 38th IEEE Conference on*, 3:2519–2523 vol.3, 1999.

[13] J. Hamberg. Controlled Lagrangians, symmetries and conditions for strong matching. In *IFAC Lagrangian and Hamiltonian Methods for Nonlinear Control*, 2000.

[14] D. D. Holm. *Geometric Mechanics, Part II: Rotating, Translating and Rolling*. Imperial College Press, 2nd edition, 2011.

[15] D. D. Holm, J. E. Marsden, and T. S. Ratiu. The Euler–Poincaré equations and semidirect products with applications to continuum theories. *Advances in Mathematics*, 137(1):1–81, 1998.

[16] D. D. Holm, T. Schmah, and C. Stoica. *Geometric mechanics and symmetry: from finite to infinite dimensions*. Oxford texts in applied and engineering mathematics. Oxford University Press, 2009.

[17] R. Ortega, J. Perez, P. Nicklasson, and H. Sira-Ramirez. *Passivity-based Control of Euler–Lagrange Systems: Mechanical, Electrical and Electromechanical Applications*. Communications and Control Engineering. Springer London, 1998.

[18] R. Ortega, M. W. Spong, F. Gomez-Estern, and G. Blankenstein. Stabilization of a class of underactuated mechanical systems via interconnection and damping assignment. *IEEE Transactions on Automatic Control*, 47(8):1218–1233, 2002.

[19] R. Ortega, A. van der Schaft, B. Maschke, and G. Escobar. Interconnection and damping assignment passivity-based control of port-controlled hamiltonian systems. *Automatica*, 38(4):585–596, 2002.

[20] S. Sastry. *Nonlinear Systems: Analysis, Stability, and Control*. Interdisciplinary Applied Mathematics. Springer New York, 1999.

[21] D. Schneider. Non-holonomic Euler–Poincaré equations and stability in Chaplygin's sphere. *Dynamical Systems*, 17(2):87–130, 2002.

[22] A. Tsolakis and T. Keviczky. Distributed IDA-PBC for a class of nonholonomic mechanical systems. *arXiv:2106.13338*, 2021.

[23] D. V. Zenkov, A. M. Bloch, N. E. Leonard, and J. E. Marsden. Matching and stabilization of low-dimensional nonholonomic systems. In *Proceedings of the 39th IEEE Conference on Decision and Control*, volume 2, pages 1289–1294 vol.2, 2000.

[24] D. V. Zenkov, A. M. Bloch, and J. E. Marsden. Flat nonholonomic matching. In *Proceedings of the 2002 American Control Conference (IEEE Cat. No.CH37301)*, volume 4, pages 2812–2817 vol.4, 2002.